ХАРАКТЕРИСТИКИ ПРОПУСКАНИЯ РУБИДИЕВОГО АТОМНОГО ОПТИЧЕСКОГО ФИЛЬТРА НА ДЛИНЕ ВОЛНЫ 780 нм, ИСПОЛЬЗУЮЩЕГО РАМАНОВСКОЕ УСИЛЕНИЕ

TRANSMISSION CHARACTERISTICS OF A RAMAN-AMPLIFIED ATOMIC OPTICAL FILTER IN RUBIDIUM AT 780 nm

© 2014 г. Wenjin Zhang, Yufeng Peng

College of Physics and Electronic Engineering, Henan Normal University, Xinxiang, China

E-mail: yufengp@sohu.com

The transmission characteristics of a Raman-amplified atomic filter that can be used to detect fairly weak signals in free-space quantum-key distribution or laser communications are analyzed and discussed in the coherent and incoherent pump fields respectively. The theoretical model for the calculation of the transmission characteristics of a ground-state Raman-amplified Faraday dispersion atomic optical filter based on Raman gain and Faraday rotation is presented. The results show that the filter in a coherent pump field can achieve higher transmission and larger tunability than that in an incoherent pump field due to elimination of pumping detuning. In addition, the filter has a large scale tunability over 3.5 GHz via the Faraday transmission peak adjusted while its bandwidth is only 66 MHz, which is useful for free-space laser communication and lidar systems.

Keywords: *atomic optical filter, Raman light amplification, Rubidium, Faraday dispersion, hyperfine structures.*

OCIS codes: 120.2440

Submitted 17.10.2013

Introduction

The Faraday anomalous dispersion optical filter (FADOF), which is based on the anomalous dispersion of Faraday rotation near the resonance lines of certain atomic vapours in a longitudinal magnetic field, have many advantages such as high transmission, narrow bandwidth, excellent out-of-band rejection and wide field of view ($\pm\pi/2$) [1–3]. It can be operated either at the line center [4–6] or in the wings [7–9] of the atomic resonance line subjected to given magnetic fields. Therefore, it has been used as a very efficient spectral-filtering device in many signal-detection systems [10–13], recently in the free-space quantum key distribution (QKD) system [14, 15], which could extract very weak signals from strong background noise and operate well in daytime and at night due to adopting the Faraday dispersive atomic filters.

A Faraday dispersive atomic filter was first described and demonstrated by Ohman (1956) [16]. The theoretical framework of a FADOF considered fine structures of atomic system was established by Yeh (1982) [1]. Yin and Shay (1991) [2] (Harrell et al., 2009 [17]) developed the theoretical framework of the FADOF based on the hyperfine structures of atomic system and ground-state transitions in the weak (any) magnetic field by using a quantum-mechanical treatment of the resonant Faraday effect. The transmission characteristics of several alkali atomic FADOFs have been observed and discussed by Menders et al. (1991, Cs D_2 line) [3], Peng et al. (1993, Rb D_2 line) [18], Hu et al. (1998, Na D lines) [5], Zhang et al. (2001, K D lines) [6], and Zielińska et al. (2012, Rb D_1 line) [19], etc. Though those filters achieved good performance, e.g., above 70% transmission (Zhang et al., 2001 [6]), and approximately 1 GHz ultra-narrow bandwidth (Zielińska et al., 2012 [19]), they couldn't have signal gain or amplification ability for the weak light. As for the weak light amplification, since the early 1990s, the mechanisms, which is based on the Raman gain attributed to stimulated Raman scattering and/or the gain from the dressed state inversion, have been extensively studied (Imamoglu et al., 1991 [20], Zibrov et al., 1995, [21], Zhu et al., 1996 [22], Zhu, 1997 [23], Wanare, 2002 [24], Kang et al., 2003 [25], Kilin et al., 2008 [26], etc.).

In 2008, Shan et al. [27] demonstrated experimentally an ultranarrow-bandwidth Raman-amplified atomic filter (RAAF) that was

a composite of a Raman light amplifier (RLA) and a dispersive atomic optical filter (i.e. FADOF), which achieved a weak light amplification of about 55 times, a bandwidth of ~ 60 MHz, and frequency tunability of ~ 1 GHz in an incoherent pump field. Compared with a conventional FADOF, the RAAF could be more suitable for operating in the free-space QKD or laser-communication systems; however, the detailed theoretical model and the analyses of transmission characteristics for this category of filter in the coherent (incoherent) pump field have not been reported.

In this paper, taking into account Raman gain mechanism in the Doppler-broadened atomic system, the theoretical model for the transmission characteristics of a Raman-amplified Faraday dispersion atomic filter is presented by basing on Raman gain involving the coupling field and pump field and Faraday rotation in the magnetic field. The gain properties, transmission and passband width of the filter subjected to the coherent and incoherent pump fields are analyzed and discussed respectively. We obtain not only the filter frequency tunability of over 3.5 GHz, which is important for free-space optical communication and lidar systems subjected to large Doppler shift. In addition, the other characteristics such as the transmission, gain, and bandwidth of the filter under the action of the coherent and incoherent pump fields are discussed.

1. Theory

The schematic diagram of the RAAF apparatus is shown in Fig. 1a. The coupling, probe (i.e. signal) and pump lasers are emitted from three different lasers, respectively. The coupling laser and probe laser have linear orthogonal polarizations and propagate in the same direction, opposite to that of the pump laser. After the three laser beams enter into the cell 1, the signal gain occurs under the combined action of coupling laser and pump laser; the probe field is amplified. The amplified probe light passes through the P4 and P5 to the Faraday cell 2, while the coupling light is distinguish by the P4. Due to the Faraday rotation effect in an axial magnetic field, the amplified signal light which frequency lies only in the transmission passband of the dispersive atomic filter, can experience a 90° rotation of the polarization and emerge apparently low absorption and high transmission.

The three-level Λ-type system for Rubidium atoms with the laser-coupled D_2 transitions is depicted in Fig. 2. Rubidium has only one stable isotope, ^{85}Rb, with the isotope ^{87}Rb, which composes almost 28% of naturally occurring Rubidium (72.17% ^{85}Rb and 27.83% ^{87}Rb). The levels $|1\rangle$, $|2\rangle$ and $|3\rangle$ represent the ground states $|5S_{1/2}, F = 2\rangle$, $|5S_{1/2}, F = 3\rangle$ and the exited state $5P_{3/2}$ of ^{85}Rb atom, and like wise, the ground

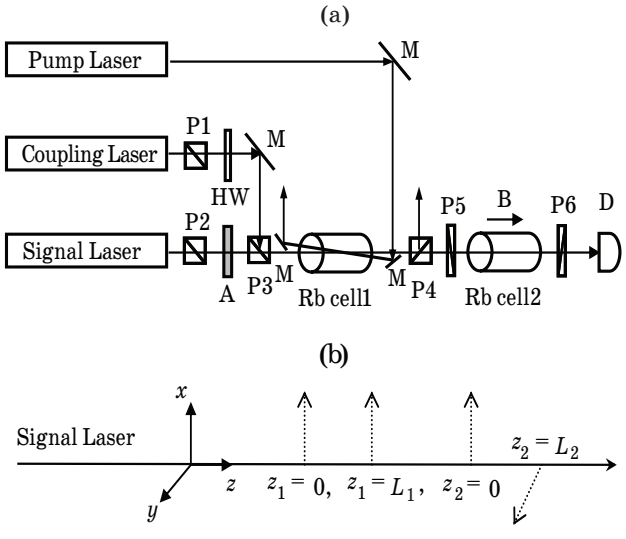

Fig. 1. Schematic diagram of the RAAF apparatus (a). P1–4 stand for polarizing beam splitters (PBS), M for a mirror, P5–6 for Glan–Thompson prism polarizers, HW for a half-wave plate, A for an attenuator, and D for a photodiode detector. Schematic of the rotation of the signal-light plane of polarization (b).

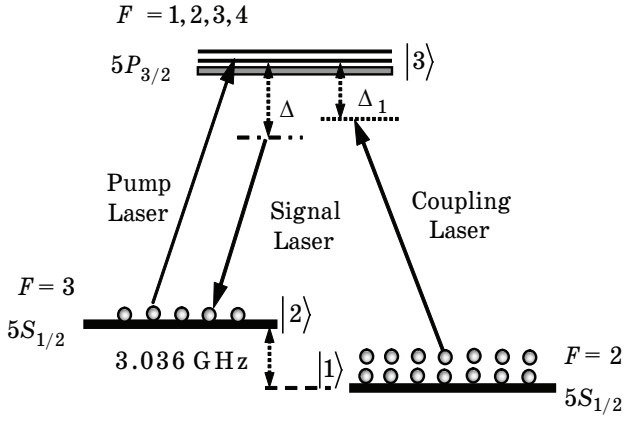

Fig. 2. ^{85}Rb far-detuned three-level Λ system. $\Delta_1(\Delta)$ is the coupling (probe) detuning. For ^{87}Rb atoms, the ground hyperfine states are $5S_{1/2}$, $F = 2$ and $5S_{1/2}$, $F = 1$, and the excited hyperfine states are $5P_{3/2}$, $F = 3, 2, 1, 0$.

states $|5S_{1/2}, F = 1\rangle$, $|5S_{1/2}, F = 2\rangle$ and the exited state $5P_{3/2}$ for ^{87}Rb atom, respectively. A coupling laser is used to connect the ground state $5S_{1/2}$ ($F = 2$ for ^{85}Rb or $F = 1$ for ^{87}Rb) $\leftrightarrow$ the excited state $5P_{3/2}$ transition, and a probe laser couples the $5P_{3/2} \leftrightarrow 5S_{1/2}$ ($F = 3$ for ^{85}Rb or $F = 2$ for ^{87}Rb) transition. A pump laser with a rate Γ is applied to the Rb $5S_{1/2}$ ($F = 3$ for ^{85}Rb or $F = 2$ for ^{87}Rb) $\leftrightarrow$ $5P_{3/2}$ transition and excites the atoms to the Rb $5P_{3/2}$ excited state.

According to above three-level system, and the electric-dipole and the rotating-wave approximations, the Hamiltonian in the interaction picture can be expressed as

$$H_1 = -\frac{\hbar}{2}\begin{bmatrix} 0 & 0 & \Omega \\ 0 & -2(\Delta_1 - \Delta) & g \\ \Omega & g & -2\Delta_1 \end{bmatrix}. \qquad (1)$$

Here Δ_1 is the detuning of the coupling beam from the atomic transition ω_{31} and Δ is the detuning of the probe field from the atomic transition ω_{32}; $\Omega = \mu_{31}E_1/\hbar$ and $g = \mu_{32}E_2/\hbar$ are the Rabi frequencies of the coupling laser (with amplitude E_1) and probe laser (with amplitude E_2); and μ_{31} and μ_{32} are the relevant dipole moments. For convenience's sake, the Rabi frequencies are taken as real parameters, and the quantum dynamics of the three-level atomic system can be described by the Liouville equation

$$\frac{\partial \rho}{\partial t} = \frac{1}{i\hbar}[H,\rho] - \frac{1}{2}\{\gamma,\rho\}. \qquad (2)$$

The full statements of Equation (2) are expressed as follows:

$$\dot{\rho}_{11} = \gamma_{31}\rho_{33} + i\Omega(\rho_{31} - \rho_{13})/2,$$

$$\dot{\rho}_{22} = -\Gamma\rho_{22} + (\Gamma + \gamma_{32})\rho_{33} + ig(\rho_{32} - \rho_{23})/2,$$

$$\dot{\rho}_{33} = \Gamma\rho_{22} - (\Gamma + \gamma_{32} + \gamma_{31})\rho_{33} + i\Omega(\rho_{13} - \rho_{31})/2 + ig(\rho_{23} - \rho_{32})/2,$$

$$\dot{\rho}_{12} = -[\Gamma/2 - i(\Delta_1 - \Delta)]\rho_{12} - ig\rho_{13}/2 + i\Omega\rho_{32}/2,$$

$$\dot{\rho}_{13} = -[\Gamma/2 + \gamma_{32}/2 + \gamma_{31}/2 - i\Delta_1]\rho_{13} - ig\rho_{12}/2 + i\Omega(\rho_{33} - \rho_{11})/2,$$

$$\dot{\rho}_{23} = -[\Gamma + \gamma_{32}/2 + \gamma_{31}/2 - i\Delta]\rho_{23} - i\Omega\rho_{21}/2 + ig(\rho_{33} - \rho_{22})/2,$$

$$\rho_{11} + \rho_{22} + \rho_{33} = 1. \qquad (3)$$

Here γ_{ij} (i, j = 1–3) are the radiative decay rates from state $|i\rangle$ to state $|j\rangle$. Since the atomic filter is used to detect a weak optical signal, we neglect the second order in g and solve Equation (3) in the steady state to get

$$\rho_{32} = \frac{ig\{(\rho_{22} - \rho_{33})(\Gamma + \gamma_{31} + \gamma_{32} - 2i\Delta_1)}{(\Gamma + \gamma_{31} + \gamma_{32} - 2i\Delta_1)} \times \times \frac{[\Gamma - 2i(\Delta_1 - \Delta)] + \Omega^2(\rho_{33} - \rho_{11})\}}{\{(2\Gamma + \gamma_{31} + \gamma_{32} + 2i\Delta)[\Gamma - 2i(\Delta_1 - \Delta)] + \Omega^2\}}, \qquad (4)$$

$$\rho_{11} = \frac{\Omega^2\Gamma(\Gamma + \gamma_{31} + \gamma_{32}) + \Omega^2(\Gamma + \gamma_{31} + \gamma_{32})(3\Gamma + \gamma_{32}) + \Gamma\gamma_{31}\left[4\Delta_1^2 + (\Gamma + \gamma_{31} + \gamma_{32})^2\right]}{+\Gamma\gamma_{31}\left[4\Delta_1^2 + (\Gamma + \gamma_{31} + \gamma_{32})^2\right]}, \qquad (5)$$

$$\rho_{22} = \frac{\Omega^2(\Gamma + \gamma_{31} + \gamma_{32}) \times \Omega^2(\Gamma + \gamma_{31} + \gamma_{32})(3\Gamma + \gamma_{32}) + \times(\Gamma + \gamma_{32}) + \Gamma\gamma_{31}\left[4\Delta_1^2 + (\Gamma + \gamma_{31} + \gamma_{32})^2\right]}, \qquad (6)$$

$$\rho_{33} = \frac{\Omega^2\Gamma \times \Omega^2(\Gamma + \gamma_{31} + \gamma_{32})(3\Gamma + \gamma_{32}) + \times(\Gamma + \gamma_{31} + \gamma_{32}) + \Gamma\gamma_{31}\left[4\Delta_1^2 + (\Gamma + \gamma_{31} + \gamma_{32})^2\right]}. \qquad (7)$$

Considering the atoms interacting with the optical field, the complex susceptibility $\chi_\pm$ at the probe field frequency can be obtained from the polarization

$$\vec{P}_\pm(z,t) = \frac{1}{2}\varepsilon_0\chi_\pm E_\pm(z,t)\hat{e}_\pm \exp[i(kz - \omega t)] + c.c. = = N_0\left(\mu_\pm\rho_{32}^{\pm}\hat{e}_\pm + c.c.\right). \qquad (8)$$

Consequently, the atomic susceptibility $\chi_{j\pm}$ of the jth $\sigma^\pm$ probe transition in the cell 1 can be written as

$$\chi_{j\pm} = \frac{\mu_{j\pm}^2 N_0}{\hbar\varepsilon_0 g_\pm}\rho_{32}^{\pm}, \qquad (9)$$

where +(−) denotes the left(right)-hand circular component, $\hbar$ is the Plank's constant divided by 2π, ε_0 is the permittivity of free space, $\mu_{j\pm}$ are the relevant dipole moments, and N_0 (with unit atom/cm^3) is the total atomic number density, given by [28]

$$\lg(N_0) = -4529.6/T - 3.991\lg T + 0.00059T + 34.8325. \qquad (10)$$

We consider the coupling laser and probe laser passing through a Doppler-broadened atomic cell 1 in the same direction. An atom moving towards the probe beam (with frequency ω_p) with velocity ν is affected by the probe frequency detuning upshifted to ($\Delta + \omega_p\nu/c$) and the frequency detuning of the coupling beam (with frequency ω_c) upshifted to $\Delta_1 + \omega_c\nu/c$. Considering that atoms are in classical thermal equilibrium with the one-dimensional Maxwellian velocity distribution of $N(\nu)d\nu = N_0\exp(-\nu^2/u^2)/(u\sqrt{\pi})d\nu$ (u is the most probable velocity and is defined as $u = (2k_BT/M)^{1/2}$), the final value of $\chi_\pm$ is obtained by integrating over the atomic velocity ν and summing over all the components of Equation (9)

$$\chi_\pm = \frac{2N_0}{\sqrt{\pi}u\hbar\varepsilon_0}\sum_j \frac{\mu_{j\pm}^2}{g_\pm}\int_{-\infty}^{+\infty}\rho_{32}^{\pm}e^{-\nu^2/u^2}\,d\nu. \qquad (11)$$

1.1. RAAF *gain*

We assume that an x-direction linearly polarized probe beam enters the atomic gas cell 1 of length L_1 (Fig. 1b) at $z_1 = 0$ and travels along the positive z-direction. The electric radiation field of the probe beam can be expressed in terms of its right- and left-circularly polarized component as

$$\vec{E}(z) = \frac{E_0}{2}\left\{\left[\exp(ik_+z) + \exp(ik\_z)\right]\hat{x} + i\left[\exp(ik_+z) - \exp(ik\_z)\right]\hat{y}\right\}\exp(-i\omega t), \qquad (11)$$

where $k_\pm$ are the circular wave-number components, given by

$$k_\pm = \frac{\omega}{c}n_\pm + \frac{i}{2}\alpha_\pm. \qquad (12)$$

By virtue of Equation (11), at $z_1 = 0$ and L_1, the x components of this probe beam may be written as

$$\vec{E}_{1x}(0) = E_0\hat{x}\exp(-i\omega t), \qquad (13)$$

$$\vec{E}_{1x}(L_1) = \frac{E_0}{2}\left[\exp(ik_+L_1) + \exp(ik\_L_1)\right]\hat{x}\exp(-i\omega t), \qquad (14)$$

respectively. The transmission coefficient of the RLA, defined by $Tr_{\mathrm{RLA}} = I_{1x}(L_1)/I_{1x}(0)$, is then given by

$$Tr_{RLA} = \frac{\left|E_{1x}(L_1)\right|^2}{\left|E_{1x}(0)\right|^2} = \exp\left(-\frac{\alpha_+ + \alpha_-}{2}L_1\right) = \exp(\bar{G}L_1), \qquad (15)$$

where $\bar{G}$ is the mean gain coefficient of the RAAF. It can be written as

$$\bar{G} = -\frac{\alpha_+ + \alpha_-}{2} = -\frac{\omega_p}{2c}\mathrm{Im}\left(\chi_+ + \chi_-\right), \qquad (16)$$

where c is the speed of light in free space.

1.2. RAAF *transmission*

When the amplified probe beam goes through the cell 1, polarizing beam splitter P4 and Glan–Thompson prism polarizer P5 to the Faraday cell 2, the x component of the polarized wave at $z_2 = 0$ is

$$\vec{E}_{2x}(0) = \vec{E}_{1x}(L_1). \qquad (17)$$

Owing to Faraday magneto-optical effect, the plane of polarization will rotate when the probe beam propagates through the cell 2 of length L_2. By virtue of Equations (11), (14) and (17), at $z_2 = L_2$, the transmitted wave which is parallel to the y-direction can be written as

$$\vec{E}_{2y}(L_2) = i\frac{E_0}{4}\left[\exp(ik_+L_1) + \exp(ik\_L_1)\right]\times \left[\exp(ik'_+L_2) - \exp(ik'\_L_2)\right]\hat{y}\exp(-i\omega t). \qquad (18)$$

The transmission Tr of the RAAF ($z_1 = 0 \to z_2 = L_2$), defined by $Tr = I_{2y}(L_2)/I_{1x}(0)$, is then given by

$$Tr = \frac{\left|E_{2y}(L_2)\right|^2}{\left|E_{1x}(0)\right|^2} = \frac{1}{2}\exp(\bar{G}L_1 - \bar{\alpha}L_2)\left[\cosh(\Delta\alpha L_2) - \cos(2\rho L_2)\right]. \qquad (19)$$

Here $\bar{\alpha}$, $\Delta\alpha$ and ρ are the mean absorption coefficient, circular dichroism, and rotatory power, respectively. They can be written as

$$\bar{\alpha} = \frac{\alpha'_+ + \alpha'_-}{2} = \frac{\omega_p}{2c}\mathrm{Im}(\chi'_+ + \chi'_-),$$

$$\Delta\alpha = \frac{\alpha'_+ - \alpha'_-}{2} = \frac{\omega_p}{2c}\mathrm{Im}(\chi'_+ - \chi'_-),$$

$$\rho = \frac{\omega_p}{2c}(n'_+ - n'_-) = \frac{\omega_p}{4c}\mathrm{Re}(\chi'_+ - \chi'_-).$$

Here $\chi'_\pm$ are the dielectric susceptibilities seen by the left and right circularly polarized components of the probe light in the magnetic field. It can be given by our previous work [28]

$$\chi'_\pm = i\frac{3\sqrt{\ln 2}e^2}{8\pi\sqrt{\pi}m\varepsilon_0\nu_{21}}\times \sum_{n,j}\frac{N_{eF}f}{\Delta\nu_{Dn}}C_FC_{3j}C_{6j}W(\delta\nu_n \pm \delta\nu_{nsj} + ia). \qquad (20)$$

where

$$C_F = (2J_1+1)(2F_1+1)(2F_2+1),$$

$$C_{3j} = \begin{pmatrix} F_2 & 1 & F_1 \\ -m_F & \pm 1 & m_F \mp 1 \end{pmatrix}^2,\ C_{6j} = \begin{Bmatrix} F_2 & 1 & F_1 \\ J_1 & I & J_2 \end{Bmatrix}^2,$$

$$W(\delta\nu_n \pm \delta\nu_{nsj} + ia) = \frac{i}{\pi}\int_{-\infty}^{+\infty} \frac{\exp(-t^2)}{\delta\nu_n \pm \delta\nu_{nsj} + ia - t}dt,$$

$$\delta\nu_n = 2\sqrt{\ln 2}\,\frac{\nu - \nu_{oF}}{\Delta\nu_{Dn}},$$

$$\delta\nu_{nsj} = 2\sqrt{\ln 2}\,\frac{\Delta\nu_{nsj}}{\Delta\nu_{Dn}},\ a = \sqrt{\ln 2}\,\frac{\Delta\nu_L}{\Delta\nu_{Dn}}.$$

Here e and m are the charge and mass of an electron, respectively, $\Delta\nu_{nsj}$ is the Zeeman hyperfine splitting depending on the external magnetic field strength, N_{eF} is the population density of the ground-state hyperfine level F of Rb atoms, f is the absorption oscillator strength of Rb D_2 line, C_{3j} is $3j$ coefficient, C_{6j} is the $6j$ coefficient, $\Delta\nu_{Dn}$ is the Doppler width, and $\Delta\nu_L$ is the Lorentz width.

Results and discussion

It is assumed that the coupling light power P_{coupling} ($P_{\text{coupling}} \approx \langle E_1 \rangle^2$) is 236 mW, and the detuned value Δ_1 of its central frequency is 4 GHz red detuned from the transition $|1\rangle = |5S_{1/2}, F = 2\rangle \rightarrow |3\rangle = |5P_{3/2}, F = 3\rangle$ of ^{85}Rb D_2 line. The coupling light also acts as the pumping laser which is ~ 1GHz detuned from the $|5S_{1/2}, F = 3\rangle \rightarrow |5P_{3/2}, F = 3\rangle$ pump transition of ^{85}Rb atom. The beam diameter d_{coupling} of the coupling light is 1.5×10^{-3} m. The gain cell length L_1 is 0.1 m and its temperature T_1 = 376 K. The Faraday cell length L_2 is 0.04 m and its temperature T_2 = 372 K. The axial magnetic strength B in the Faraday cell is 0.0205 T. According to Equation (19), the peak transmission of the Raman-amplified atomic filter as a function of probe detuning from a resonance transition for $5S_{1/2}(F = 3) \rightarrow 5P_{3/2}$ of ^{85}Rb in an incoherently pumped field (pump detuning $\Delta_p \approx -1$ GHz) is shown in Fig. 3. It can be found that the RAAF displays a single dominant peak with transmission of 18.4 (corresponding to $\bar{G} = 29$) at 4.0 GHz relative to the absorption peak 1a with FWHM (full width at half maximum) of 66 MHz. The analytical results correspond greatly to the experimental results carried out by Shan [27].

Fig. 4a, b show an atomic absorption spectrum in cell 1 and a typical transmission spectrum

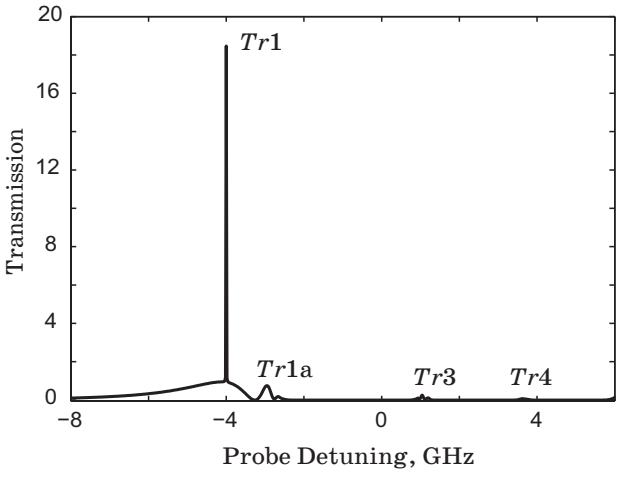

Fig. 3. The transmission of the Raman-amplified atomic filter versus the probe detuning. P_{coupling} = 236 mW, $d_{\text{coupling}} = 1.5\times10^{-3}$ m, T_1 = = 376 K, T_2 = 372 K, L_1 = 0.1 m, L_2 = 0.04 m, B = 0.0205 T and $\Delta_1 = -4.0$ GHz, $\Delta_p = -0.964$ GHz.

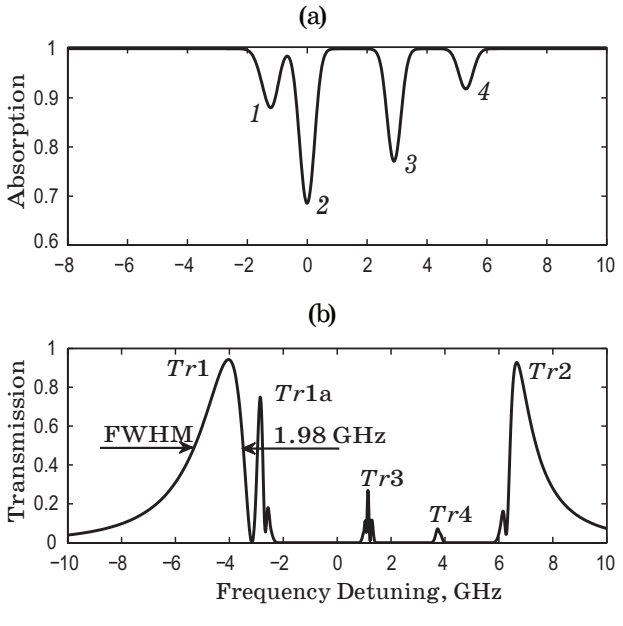

Fig. 4. The atomic absorption spectrum in cell 1 without coupling light at room temperature (293 K) (a). This spectrum is used to calibrate the transmission spectrum of the filters. The absorption peaks *1*, *2*, *3*, and *4* correspond to the ^{87}Rb $|5S_{1/2}, F = 2\rangle \rightarrow |5P_{3/2}\rangle$, ^{85}Rb $|5S_{1/2}, F = 3\rangle \rightarrow |5P_{3/2}\rangle$, ^{85}Rb $|5S_{1/2}, F = 2\rangle \rightarrow |5P_{3/2}\rangle$ and ^{87}Rb $|5S_{1/2}, F = 1\rangle \rightarrow |5P_{3/2}\rangle$ transitions, respectively. The position of absorption peak *2* is set to zero detuning point. The transmission spectrum of the dispersive atomic filter without the coupling light (b). T_1 = 376 K, T_2 = 372 K, L_1 = 0.1 m, L_2 = 0.04 m and B = 0.0205 T.

of the FADOF in cell 2 without coupling light, respectively. The FADOF displays a 1.98 GHz bandwidth (FWHM) at a maximum peak ($Tr1$) transmittance of 94.6%. It should be noted that the Rb-FADOF possesses a secondary maximum peak $Tr2$ in the strong magnetic field [9], while it doesn't emerge in reference [27] mainly because the transmission frequency of peak $Tr2$ is beyond the scan range of signal-light frequency (≈15 GHz).

Fig. 5a, b represent the gain coefficient, transmission and FWHM of the RAAF in the incoherent pump field [27] as a function of coupling-light power, respectively. It can be seen that with the coupling-light power (P_{coupling}) increasing from 60 to 95 mW, the RAAF can achieve a larger gain, higher transmission and a narrower bandwidth. When P_{coupling} varies from 95 to 500 mW, the filter can obtain an ultra-narrow bandwidth of 66 MHz and the transmission coefficient of over 2.5. It is worth mentioning that the saturation of transmission coefficient appears when P_{coupling} attains to approximatelly 472 mW, as shown in Fig. 5a, which means that too larger coupling-laser power is unnecessary to get a higher transmission.

The outstanding characteristic of the RAAF is the light amplification by comparison with traditional FADOFs. According to Equations (6) and (7), we can get

$$\frac{\rho_{33}}{\rho_{22}} = \frac{\Gamma}{\Gamma + \gamma_{32}} < 1. \qquad (18)$$

It is easily found that the signal gain or amplification in a RAAF does not require population inversion in the relevant atomic states $|3\rangle$ and $|2\rangle$. It can be induced by the stimulated Raman scattering $|1\rangle \to |3\rangle \to |2\rangle$ in which the atoms absorb a coupling-laser photon and then emit a probe-laser photon.

When the pump laser is provided in Fig. 1 and the pump beam is on resonance with $|5P_{1/2}, F = 3\rangle \to |5P_{3/2}, F = 3\rangle$ transition of ^{85}Rb atom, the transmission and FWHM of the RAAF as a function of the pump rate in the coherent pump field is given in Fig. 6. It can be found that the peak transmission increases with continually increasing of the pump rate. When the coupling-light power is 60 mW, and the pump-laser rate is $4.5\gamma_{32}$ (the corresponding pump-laser power ~2.85 mW, $\gamma_{32} \approx 19.06$ MHz), the RAAF displays a peak transmission of 11.2 and an ultra-narrow bandwidth of 66 MHz, and while the equal coupling-light power is supplied in the incoherent pump field, the filter only obtains a peak transmission of 1.36 with the bandwidth of over 1 GHz (Fig. 5a, b) due to the larger pumping detuning (≈ −1 GHz) that corresponds to a lower pump rate (≈$0.29\gamma_{32}$). To obtain 11.2 transmission in the incoherent pump field, the coupling-light power required is up to 180 mW (Fig. 5a), which is triple of that in the coherent pump field. By comparing transmission characteristics in the coherent with incoherent pump fields, it is easy to find that the filter in a coherent pump field can be more effective to obtain higher peak transmission and narrower bandwidth.

The transmission, FWHM and peak detuning of the RAAF as a function of coupling-light

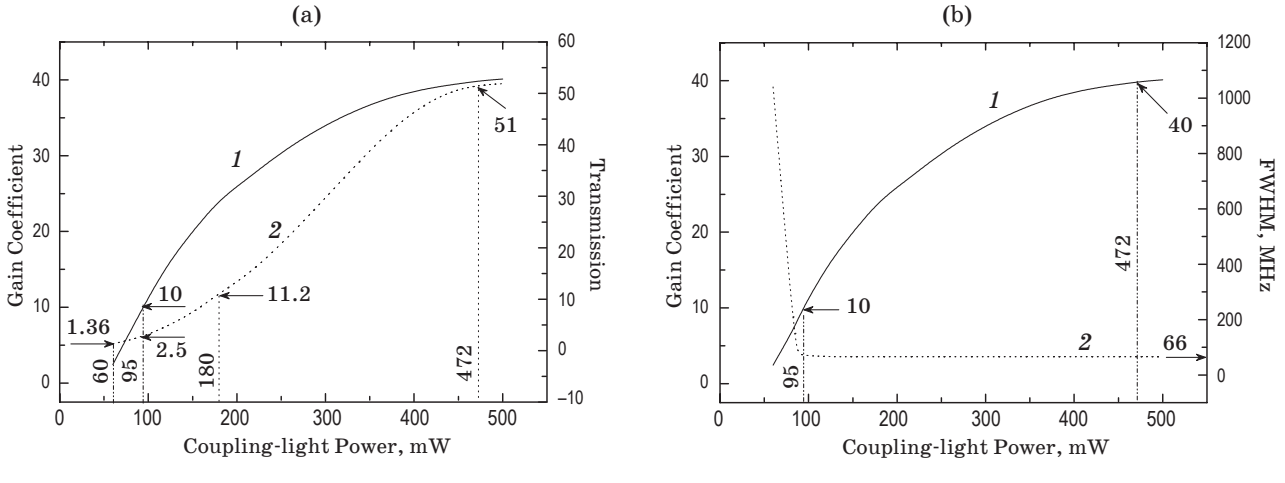

Fig. 5. Gain coefficient (*1*) and transmission (*2*) (a), gain coefficient (*1*) and FWHM of the RAAF (*2*) as a function of the coupling-light power in the incoherent pump field (b). $d_{\text{coupling}} = 1.5\times10^{-3}$ m, $\Delta = \Delta_1 = -4.0$ GHz, $\Delta_p = -0.964$ GHz, and other parameters are the same as in Fig. 4b.

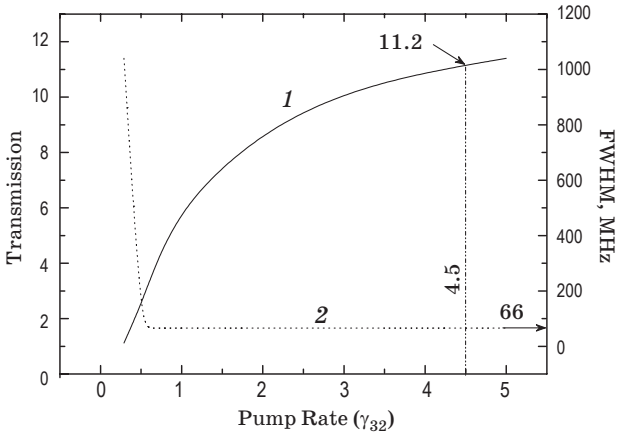

Fig. 6. The transmission (*1*) and FWHM (*2*) of the RAAF as a function of the pump rate in the coherent pump field. $P_{coupling}$ = 60 mW, $d_{coupling} = d_{pump} = 1.5\times10^{-3}$ m, $\Delta = \Delta_1 = -4.0$ GHz, Δ_p = 0, and other parameters are the same as in Fig. 4b.

detuning Δ_1 in the incoherent pump field are shown in Fig. 7a, b. From these figures, it can be seen that the largest peak transmission appears at $\Delta \approx -3.88$ GHz, and the effective tunable range of transmission frequency is ~1.54 GHz due to two-photon resonance requirement in the Raman scattering process ($\Delta = \Delta_1$). Within this tunable range, the transmission bandwidth is kept as 66 MHz with the transmission of over 2.5, and out of the range, the bandwidth is increased quickly to gigahertz level with the reduction of transmission, so that the filter can't realize an effective signal amplification filtering. For the above tuning, the transmission frequency of the RAAF is tuned only near a Faraday transmission peak $Tr1$ (at $\Delta = -4.0$ GHz, Fig. 4b), and this gives rise to the limited tunability of the filter.

The realization of the filter's tunability is also achieved by changing the position of the Faraday transmission peak. It is well known that the transmission peak of FADOF can be tuned through changing the magnetic field strength or Faraday cell temperature. As an example, at 388 K, with a Rubidium cell (0.04 m in length) in an axial magnetic field of 0.0211 T, the transmission spectrum of a FADOF is shown in Fig. 8. It is easy to see from Fig. 4b and 8 that the transmission peak $Tr1$ is tuned ~ 2 GHz.

The dependence of transmission, FWHM and peak detuning of the RAAF in a new Faraday transmission peak $Tr1$ (Fig. 8) on coupling-light detuning in the incoherent pump field is shown in Fig. 9a, b. In which, the filter shows an effective frequency tunability of ~ 0.6 MHz under 66 MHz bandwidth because of large pump detuning. When a coherent pump field with a rate $\Gamma = 3\gamma_{32}$ is applied, the RAAF's tunability can reach ~ 1.75 GHz with a bandwidth of 66 MHz, as shown in Fig. 10a, b. It can be seen obviously from Fig. 7, 9 and 10 that the RAAF in the coherent pump field can achieve a larger tunability (~ 3.53 GHz, ~ $-3.47 \rightarrow$ $\rightarrow$ ~ -7 GHz) than that in the incoherent pump field by means of the Faraday transmission peak adjusted.

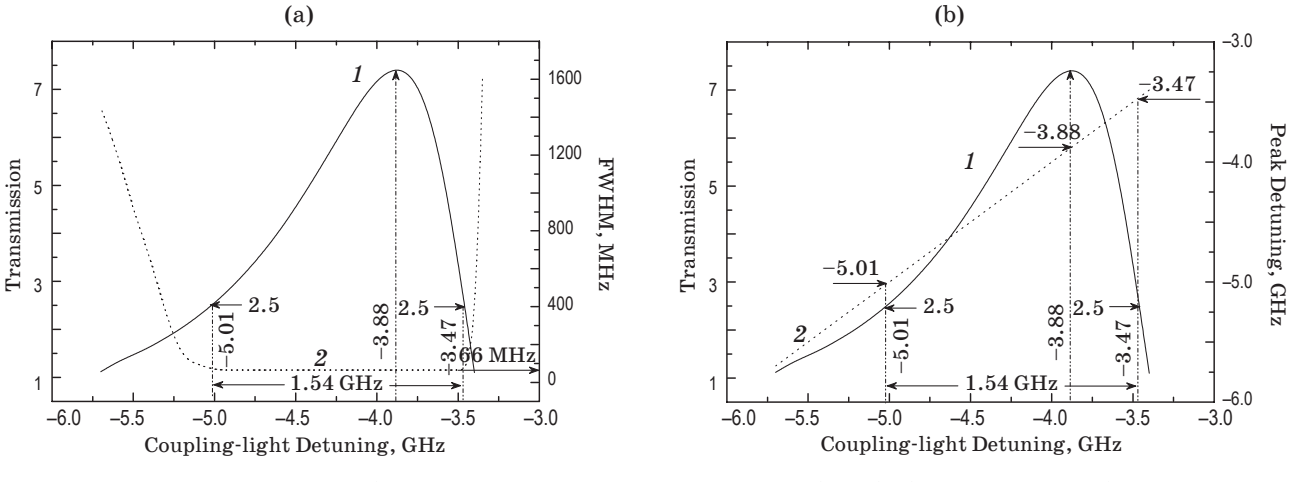

Fig. 7. Transmission (*1*) and FWHM (*2*) (a), transmission (*1*) and peak detuning (*2*) of the RAAF as a function of coupling-light detuning in the incoherent pump field (b). $P_{coupling}$ = 150 mW, $d_{coupling} = 1.5\times10^{-3}$ m, $\Delta_p = \Delta_1 + \omega_{21}$, and other parameters are the same as in Fig. 4b.

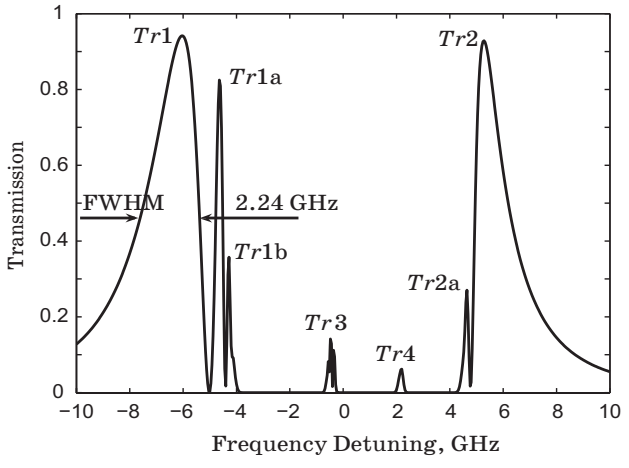

Fig. 8. Rb FADOF transmission versus signal laser frequency. $T_2 = 388$ K, $L_2 = 0.04$ m, and $B = 0.0211$ T.

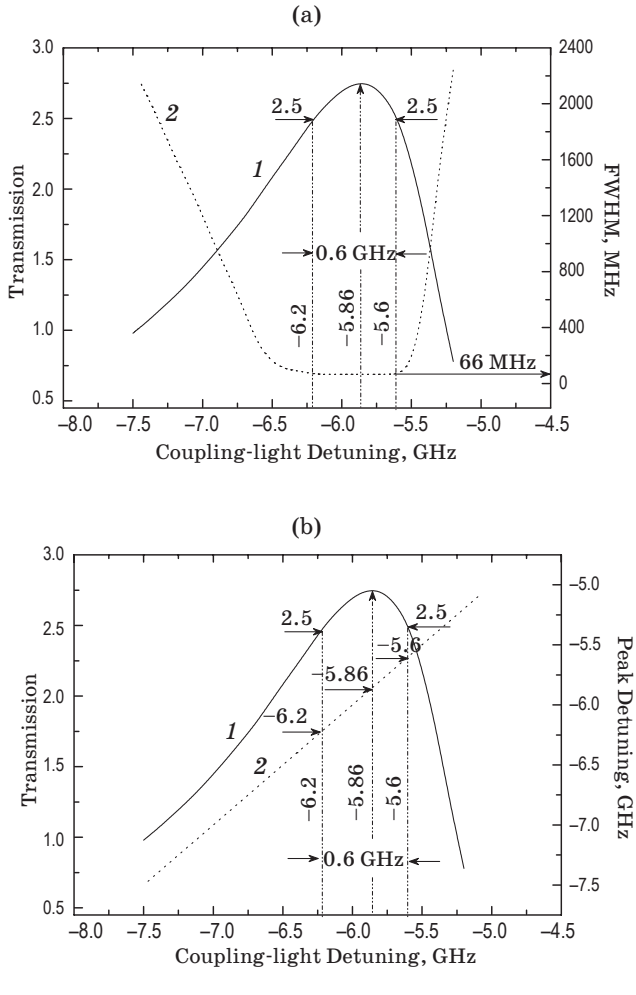

Fig. 9. Dependence of transmission (*1*) and FWHM (*2*) (a), transmission (*1*) and peak detuning (*2*) of the RAAF on the coupling-light detuning in the incoherent pump field (b). $P_{\text{coupling}} = 150$ mW, $d_{\text{coupling}} = 1.5\times10^{-3}$ m, $\Delta_p = \Delta_1 + \omega_{21}$, $T_1 = 376$ K, $T_2 = 388$ K, $L_1 = 0.1$ m, $L_2 = 0.04$ m, $B = 0.0211$ T.

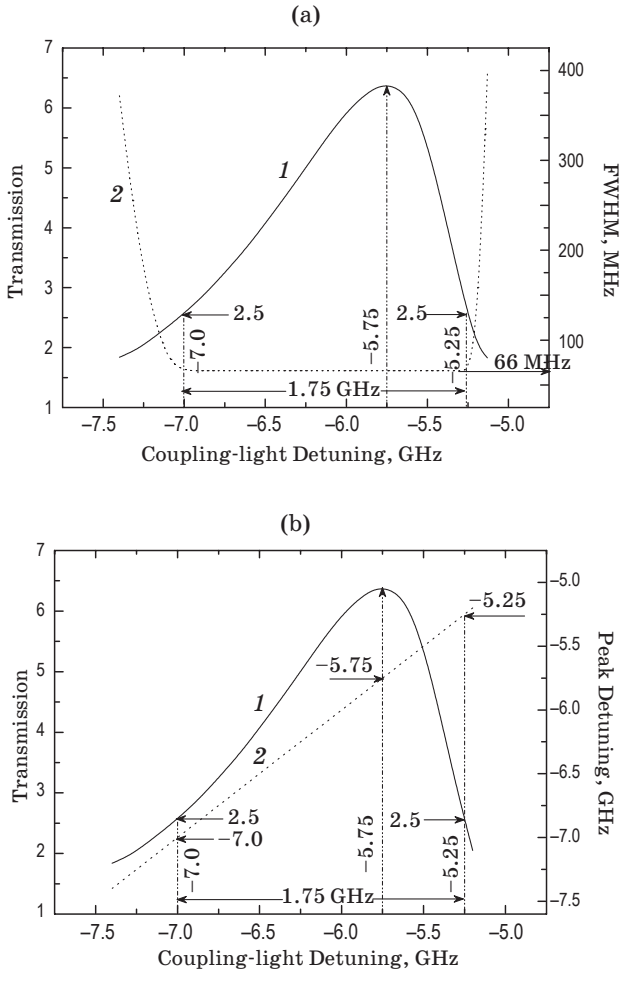

Fig. 10. Transmission (*1*) and FWHM (*2*) (a), transmission (*1*) and peak detuning (*2*) of the RAAF as a function of the coupling-light detuning in the coherent pump field (b). $P_{\text{coupling}} = 150$ mW, $d_{\text{coupling}} = d_{\text{pump}} = 1.5\times10^{-3}$ m, $\Gamma = 3\gamma_{32}$, $\Delta_p = 0$, $T_1 = 376$ K, $T_2 = 388$ K, $L_1 = 0.1$ m, $L_2 = 0.04$ m, $B = 0.0211$ T.

Conclusion

In conclusion, we have presented a theoretical model for a ground-state Raman-amplified Faraday dispersion atomic filter based on the Raman light gain and Faraday rotation in Rubidium at 780 nm. By comparing transmission characteristics of the filter in the coherent and incoherent pump fields, we find that the filter in a coherent pump field has a higher peak transmission and a larger tunability than that in an incoherent pump field, which is of great significance for practical applications of the Raman-amplified atomic filter. Moreover, the filter can achieve the peak transmission of over 10, an ultra-narrow

bandwidth of 66 MHz and the tunability of no less than 3.5 GHz in the coherent pump field, which is very helpful for us to improve the detection of weak signals in free-space optical communication, QKD and lidar systems subjected to large Doppler shift. This model, which includes weak light amplification, is expected to be helpful in investigating the performances of Raman-amplified atomic filters for other atomic lines.

The authors would like to acknowledge the support from the National Natural Science Foundation of China (grant 61077037).

* * * * *

REFERENCES

1. *Yeh P.* Dispersive magnetooptic filters // Appl. Opt. 1982. V. 21. № 11. P. 2069–2075.
2. *Yin B., Shay T.M.* Theoretical model for a Faraday anomalous dispersion optical filter // Opt. Lett. 1991. V. 16. № 20. P. 1617–1619.
3. *Menders J., Benson K., Bloom S.H., Liu C.S., Korevaar E.* Ultranarrow line filtering using a Cs Faraday filter at 852 nm // Opt. Lett. 1991. V. 16. № 11. P. 846–848.
4. *Chen H., She C.Y., Searcy P., Korevaar E.* Sodium-vapor dispersive Faraday filter // Opt. Lett. 1993. V. 18. № 12. P. 1019–1021.
5. *Hu Z., Sun X., Liu Y., Fu L., Zeng X.* Temperature properties of Na dispersive Faraday optical filter at D_1 and D_2 line // Opt. Commun. 1998. V. 156. № 4–6. P. 289–293.
6. *Zhang Y., Jia X., Ma Z., Wang Q.* Potassium Faraday optical filter in line-center operation // Opt. Commun. 2001. V. 194. № 1–3. P. 147–150.
7. *Dick D.J., Shay T.M.* Ultrahigh-noise rejection optical filter // Opt. Lett. 1991. V. 16. № 11. P. 867–869.
8. *Dressler E.T., Laux A.E., Billmers R.I.* Theory and experiment for the anomalous Faraday effect in potassium // J. Opt. Soc. Am. B. 1996. V. 13. № 9. P. 1849–1858.
9. *Hu Z., Sun X., Zeng X., Peng Y., Tang J. Zhang L., Wang Q., Zheng L.* Rb 780 nm Faraday anomalous dispersion optical filter in a strong magnetic field // Opt. Commun. 1993. V. 101. № 3–4. P. 175–178.
10. *Tang J., Wang Q., Li Y., Zhang L., Gan J., Duan M., Kong J., Zheng L.* Experimental study of a model digital space optical communication system with new quantum devices // Appl. Opt. 1995. V. 34. № 15. P. 2619–2622.
11. *Fricke-Begemann C., Alpers M., Höffner J.* Daylight rejection with a new receiver for potassium resonance temperature lidars // Opt. Lett. 2002. V. 27. № 21. P. 1932–1934.
12. *Höffner J., Fricke-Begemann C.* Accurate lidar temperatures with narrowband filters // Opt. Lett. 2005. V. 30. № 8. P. 890–892.
13. *Popescu A., Walldorf D., Schorstein K., Walther T.* On an excited state Faraday anomalous dispersion optical filter at moderate pump powers for a Brillouin-lidar receiver system // Opt. Commun. 2006. V. 264. № 2. P. 475–481.
14. *Buttler W.T., Hughes R.J., Kwiat P.G., Lamoreaux S.K., Luther G.G., Morgan G.L., Nordholt J.E., Peterson C.G., Simmons C.M.* Practical free-space quantum key distribution over 1 km // Phys. Rev. Lett. 1998. V. 81. № 15. P. 3283–3286.
15. *Shan X., Sun X., Luo J., Tan Z., Zhan M.* Free-space quantum key distribution with Rb vapor filters // Appl. Phys. Lett. 2006. V. 89. № 19. P. 191121–191123.
16. *Ohman Y.* On some new auxiliary instruments in astrophysical research VI. A tentative monochromator for solar work based on the principle of selective magnetic ratation // Stockholms Obs. Ann. 1956. V. 19. № 4. P. 9–11.
17. *Harrell S.D., She C.Y., Yuan T., Krueger D.A., Chen H., Chen S.S., Hu Z.L.* Sodium and potassium vapor Faraday filters revisited: theory and applications // J. Opt. Soc. Am. B. 2009. V. 26. № 4. P. 659–670.
18. *Peng Y.F., Tang J.X., Wang Q.J.* Study of Faraday anomalous dispersion spectra of the hyperfine structure of Rb D_2 lines // Acta Phys. Sin. (Overseas Edn). 1993. V. 2. № 1. P. 1–8.
19. *Zielinska J.A., Beduini F.A., Godbout N., Mitchell M.W.* Ultranarrow Faraday rotation filter at the Rb D_1 line // Opt. Lett. 2012. V. 37. № 4. P. 524–526.
20. *Agarwal G.S.* Origin of gain in systems without inversion in bare or dressed states // Phys. Rev. A. 1991. V. 44. № 1. P. R28–R30.

21. *Zibrov A.S., Lukin. M.D., Nikonov D.E., Hollberg L., Scully M.O., Velichansky V.L., Robinson H.G.* Experimental demonstration of laser oscillation without population inversion via quantum interference in Rb // Phys. Rev. Lett. 1995. V. 75. № 8. P. 1499–1502.

22. *Zhu Y., Lin J.* Sub-Doppler light amplification in a coherently pumped atomic system // Phys. Rev. A. 1996. V. 53. № 3. P. 1767–1774.

23. *Zhu Y.* Light amplification mechanisms in a coherently coupled atomic system // Phys. Rev. A. 1997. V. 55. № 6. P. 4568–4575.

24. *Wanare H.* Gain without population inversion in V-type systems driven by a frequency-modulated field // Phys. Rev. A. 2002. V. 65. № 3. P. 033417–033427.

25. *Kang H., Wen L., Zhu Y.* Normal or anomalous dispersion and gain in a resonant coherent medium // Phys. Rev. A. 2003. V. 68. № 6. P. 063806–063810.

26. *Kilin S.Y., Kapale K.T., Scully M.O.* Lasing without inversion: counterintuitive population dynamics in the transient regime // Phys. Rev. Lett. 2008. V. 100. № 17. P. 173601–173604.

27. *Shan X., Sun X., Luo J., Zhan M.* Ultranarrow-bandwidth atomic filter with Raman light amplification // Opt. Lett. 2008. V. 33. № 16. P. 1842–1844.

28. *Peng Y., Zhang W., Zhang L., Tang J.* Analyses of transmission characteristics of Rb, ^{85}Rb and ^{87}Rb Faraday optical filters at 532 nm // Opt. Commun. 2009. V. 282. № 2. P. 236–241.